Nonlinear Absorption of High Power Free-Electron-Laser-Generated Microwaves at Electron Cyclotron Resonance Heating Frequencies in the MTX Tokamak

S. L. Allen, M. D. Brown, J. A. Byers, T. A. Casper, B. I. Cohen, R. H. Cohen, M. E. Fenstermacher, J. H. Foote, E. B. Hooper, C. J. Lasnier, P. Lopez, M. A. Makowski, M. M. Marinak, W. H. Meyer, J. M. Moller, W. M. Nevins, B. W. Rice, T. D. Rognlien, G. R. Smith, B. W. Stallard, E. T. Scharlemann, K. I. Thomassen, and R. D. Wood

Lawrence Livermore National Laboratory, Livermore, California 94551

K. Hoshino,[1] K. Oasa,[1] T. Oda,[2] K. Odajima,[1] T. Ogawa,[1] and T. Ohgo,[3]

[1]*Japan Atomic Energy Research Institute, Naka, Japan*

[2]*Hiroshima University, Hiroshima, Japan*

[3]*Fukuoka University of Education, Fukuoka, Japan*

(Received 6 May 1993)

We report the first measurements of single-pass propagation of intense (>1-GW, 20-ns) microwaves through a high-density $[n_e=(0.5\text{–}2.4)\times10^{20}\ \mathrm{m}^{-3}]$ tokamak plasma at 140 GHz, the fundamental electron cyclotron resonance frequency. Compared with low-power pulses, these free-electron-laser-generated intense pulses were not as strongly absorbed by the plasma, in agreement with predictions of nonlinear theory. Enhanced absorption of intense pulses was achieved by increasing the gradient in the parallel index of refraction ($N_\parallel$) of the microwave beam.

PACS numbers: 52.50.Gj, 52.35.Mw, 52.75.Ms

The decrease of the Coulomb collision frequency with increasing temperature places a fundamental limitation on Ohmic heating in toroidally confined plasmas. Consequently, a major thrust of controlled thermonuclear fusion research has been the development of auxiliary heating techniques for both ions and electrons. In many cases, these same techniques can be used to drive plasma current and provide local control of plasma profiles. The purpose of the microwave tokamak experiment (MTX) is to study one particular type of electron heating in tokamaks: electron cyclotron resonance heating (ECRH). The major advantage of ECRH is that very localized electron heating is achieved, as absorption occurs where the wave frequency equals the local electron cyclotron frequency f_{ce}= 28 GHz/T (140 GHz at 5 T for MTX).

In the MTX experiment, we measured for the first time the interaction of very intense (>1-GW, 20-ns) microwave pulses with a high-density $[n_e = (0.5\text{–}2.4) \times 10^{20}\ \mathrm{m}^{-3}]$ plasma confined in a high-toroidal-field tokamak (B_T = 5 T). These pulses were generated by a free electron laser (FEL) [1] and represent the highest peak power generated to date at 140 GHz. The use of an FEL for ECRH has several technological advantages, including the potential of frequency sweeping (±10%) to vary the heating zone [2] and the ability to generate high-frequency microwaves for heating at high density. ECRH with an FEL also makes possible several novel heating and current drive schemes [3].

For comparison, we have also performed more conventional ECRH experiments with moderate-power, long-pulse (200-kW, ~100-ms) microwaves generated by a gyrotron. These results, discussed in detail elsewhere [4], are similar to those obtained on other tokamaks, such as DIII-D [5] and T-10 [6]. In general, these experiments show efficient heating and are in agreement with thoroughly developed linear theories of ECRH [7].

The ECRH theory has been extended to the nonlinear (high-microwave electric field) regime [8] relevant to the FEL experiments. A simple phase space picture of the nonlinear effect is that electrons are strongly heated by the intense microwave beam and become nonlinearly trapped near the cyclotron resonance. While trapped, they exhibit adiabatic motion with a concomitant reduction in opacity compared to the linear theory. However, the nonlinear opacity increases with electron temperature and plasma size [8,9], so that estimates for high-temperature reactor-grade plasmas indicate good absorption of these intense pulses. The nonlinear theory also predicts the generation of energetic electrons (5–25 keV in MTX). Theoretical estimates of the magnitude of other mechanisms that could degrade the absorption, such as parametric effects [9], indicate that these are not large in MTX. In all, theory predicts that the MTX FEL experiments should show significant, observable differences in absorption from linear theory, and heating by intense pulses can be an attractive option for future tokamaks.

In the MTX experiment, a microwave source (FEL or gyrotron) is coupled to the MTX tokamak via a quasi-optical microwave transport system. The FEL, an improved version of the system developed by the Beam Research Group at LLNL [10–12], consists of the ETA-II accelerator with improved electron beam quality [1] and a steady-state tunable wiggler [13]. Microwave pulses with peak powers in the range of 1–2 GW were generated by the FEL. The transport system was constructed so that horizontally polarized microwaves (ordinary mode)

0031-9007/94/72(9)/1348(4)$06.00

were launched into the plasma from the low-field side of the tokamak (outside). Peak powers up to 1.4 GW were measured by a calorimeter at MTX, consistent with theoretical estimates (89%) of the transmission of the transport system. Measurements of the vacuum FEL-generated electric field [14] were also consistent with this power level. The MTX transmission experiments were all single pulse (FWHM $\simeq$20 ns); multiple-pulse bursts of microwaves were generated after the conclusion of MTX experiments [15].

Figure 1 presents representative plasma data from a discharge used for FEL experiments. The plasma current is 200 kA, the electron density is 5×10^{19} m^{-3}, and the central electron temperature is $\sim$1.2 keV. The data from the x-ray diagnostic located at the FEL port are also shown; the FEL pulse was injected at approximately 200 ms. The x-ray sampling rate is increased during the time of the FEL pulse; the expanded data for three spatial chords are shown. Note the very localized nature of the x-ray response: only the detector viewing near the plasma axis ($r = -1.4$ cm) shows heated electrons.

The microwave transmission was measured in the MTX tokamak with a 48-channel electronic calorimeter mounted on the inside wall of the machine. The microwave beam enters the tokamak from the outside, interacts with the plasma (both absorption and refraction), and is then measured by the calorimeter channels. Three thermistors (distributed toroidally) are mounted on each of the 19 silicon carbide tiles (distributed poloidally); 48 of these channels are connected to the electronics. The tiles, with high absorption at microwave frequencies, are shielded from plasma radiation by a sandwich of several materials. During the four years of MTX experiments, some channels failed, resulting in about 28 useable channels at the time of these experiments. The highest concentration of useable channels was near the plasma axis; experimentally we found that this is also where the signals are the largest. For these reasons, the most reliable data were obtained near the plasma axis.

For comparison with theory, we have defined the core transmission as the processed signal from the sum of the channels on the three central calorimeter tiles ($\pm$3 cm near the axis of the machine). The transmission was obtained from the temperature rise with plasma normalized to the output power of the FEL divided by the no-plasma normalized signal. Figure 2 shows the core ($\pm$ 3 cm) transmission data $T_{\rm FEL}$ from calorimetry as a function of peak electron density (from inverted interferometer line-density profiles) for FEL input powers in the range of 0.8–1.4 GW (red circles). For comparison, data from low-power $T_{\rm low}$ ($\sim$3 kW, i.e., master oscillator only with no FEL gain) are shown (green diamonds). Note that $T_{\rm FEL} > T_{\rm low}$ for all densities, demonstrating the nonlinear behavior. Theoretical predictions for both nonlinear (red) and linear (green) theory are included.

The linear theoretical calculation is the product of transmission times refraction; the latter is calculated from a ray-tracing code [16] using electron density pro-

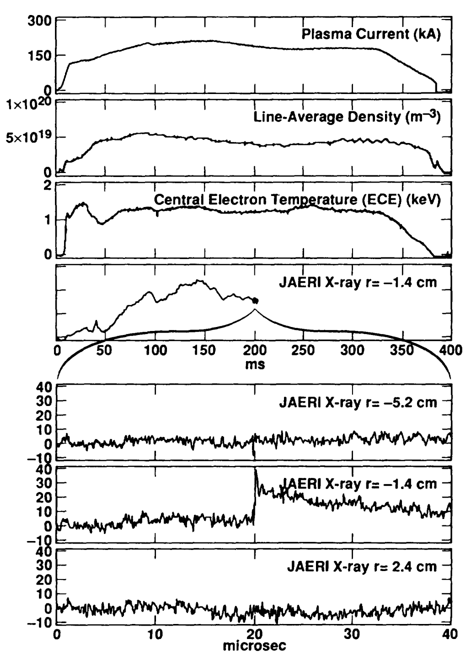

FIG. 1. The plasma current, electron density, and central T_e from a representative discharge used for FEL absorption experiments. The FEL is injected at 200 ms; the expanded x-ray data show a spatially localized response.

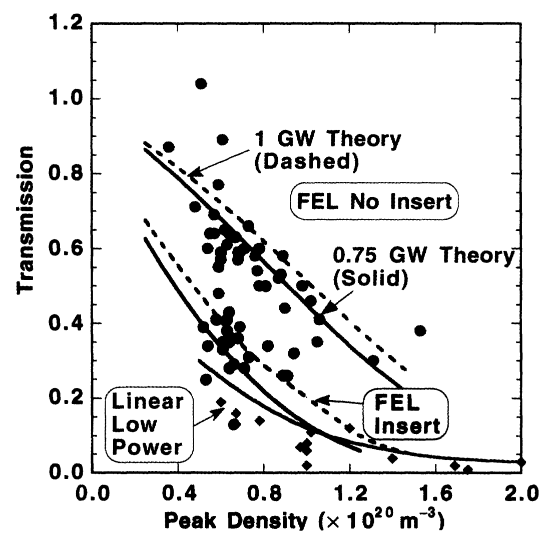

FIG. 2. The FEL high-power core transmission data (red circles) are greater than low-power data (green diamonds), demonstrating nonlinear absorption. Theoretical predictions of the FEL transmission without the insert (red: 1 GW, dashed; 0.75 GW, solid) compare well with the FEL data. An insert increases the $N_{\|}$ gradient of the microwave beam, thereby decreasing the experimentally measured transmission (blue circles), in agreement with nonlinear theory (blue: 1 GW, dashed; 0.75 GW, solid). The insert data and theory approach the linear theory (green line).

files measured with a 15-chord far-infrared interferometer. The reduction in transmission due to refraction is about 0.1, 0.2, and 0.5 at a peak density of 0.5, 1.0, and 1.5×10^{20} m^{-3}, respectively, for typical MTX profiles. There is good agreement between the linear theory $T_{\rm lin}^{\rm theory}$ (green line) and the $T_{\rm low}$ (green diamonds) data. Previous experiments performed at ~200 kW with a gyrotron on MTX showed similar agreement [4]. Also, earlier measurements with the FEL [11,12] (at 100–150 MW) were consistent with linear theory, as predicted.

In the nonlinear theoretical calculations for the FEL case, a refraction-modified on-axis electric field was used in the orbit-following code [17]; the transmission was then further reduced by refraction from the magnetic axis to the wall. Curves for 1 GW (dashed red) and 0.75 GW (solid red) are shown; the latter curve is approximately the average power obtained from the time history of the FEL pulse. Note there is good agreement between the nonlinear theory curve $T_{\rm FEL}^{\rm theory}$ (0.75 GW, red solid) and the data $T_{\rm FEL}$ (red circles), indicating that the theory accurately models the data. The estimated measurement error of the $T_{\rm FEL}$ data is on the order of 10%, less than the observed scatter in the data in Fig. 2. We have attempted to ascertain power and electron temperature scalings from the calorimeter data; we also have time-resolved transmission measurements from an on-axis microwave horn. However, due to the scatter in both data sets we could not derive any significant scalings with input power (0.7–1.4 GW) or electron temperature (0.8–1.4 keV). The scatter is not well understood, but may be due to variations in undetermined plasma effects (e.g., scattering from edge plasma fluctuations).

The nonlinear theory also predicts that the opacity increases with the gradient in $N_{\parallel}$ [18]. To test this theory, we installed a corrugated-wall, tapered insert in the entrance port to the MTX tokamak. By tapering the beam to small toroidal dimension at the output of the taper, diffraction spreads the beam in the toroidal direction. The on-axis beam size is similar in the two cases, but the $N_{\parallel}$ (toroidal) spread is increased from $\Delta N_{\parallel} = 0.1$ without the insert to 0.35 with the insert. The beam shape with the insert was verified by low-power side-lab experiments.

The theoretical predictions for the transmission with the insert $T_{\rm insert}^{\rm theory}$ are also plotted in Fig. 2. Again, theory curves for 1.0 GW (blue dashed) and 0.75 GW (blue solid) are presented. Note that the theoretical transmission is reduced for the case with the insert: $T_{\rm insert}^{\rm theory}$(blue) $< T_{\rm FEL}^{\rm theory}$ (red). Furthermore, the insert case approaches the linear prediction $T_{\rm lin}^{\rm theory}$ (theory indicates that the nonlinear opacity can even exceed the linear opacity). The core transmission with the insert $T_{\rm FEL}^{\rm insert}$ was also measured with the calorimeter and the data are presented in Fig. 2 (blue circles). Again, there is good agreement between the theory (blue lines) and the data (blue circles); these data are also approaching the low-power data values (green diamonds) and the linear theory (green line).

We have also performed a comparison of the total calorimeter data with and without the tapered wall insert. Two-dimensional spline fits were generated, and to increase the signal-to-noise at the edge of the calorimeter, several shots with similar peak electron densities were summed. These data showed the same trend as the core data: the transmission data with the insert were lower than without the insert by approximately a factor of 2. Error bars were estimated to be on the order of 25%. However, the absolute values of the transmission were uniformly lower than the core values discussed above. This is caused by the fact that the microwaves, which are refracted to the upper and lower regions of the plasma, are not measured in the regions where there are no working calorimeter channels. This is consistent with the fact that the agreement between the total calorimeter data and theory is poorer at higher plasma densities, where refraction plays a more important role.

During FEL experiments, we have observed energetic electrons with soft x-ray, electron cyclotron emission (ECE), and Thomson scattering diagnostics. The change in the electron distribution function due to the FEL pulse was measured by the Thomson scattering diagnostic located 120° toroidally away from the FEL port; these data are presented in Fig. 3. The photon count as a function of wavelength for data with (solid circles) and without (open diamonds) the FEL are shown; six shots have been averaged for each set to increase the signal-to-noise ratio. The dashed curve shows the expected signal for a Maxwellian electron distribution at the measured plasma electron temperature (1.5 keV) corrected for relativistic effects; note the FEL data deviate from this curve at high energies, signifying the presence of energetic electrons. The orbit-following code [17] was used to calculate the effect of the FEL pulse on the electron distribution function, taking into account the location of

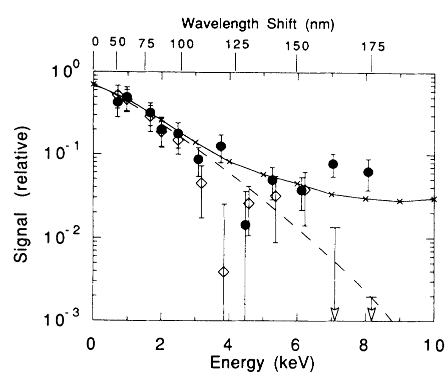

FIG. 3. Thomson scattering data with (solid circles) and without (open diamonds) the FEL; note the presence of high-energy electrons in the FEL case near 7–8 keV. Plasma parameters were T_e=1.5 keV, $n_e = 0.65 \times 10^{20}$ m^{-3}, and 1 GW FEL power. The Maxwellian distribution (dashed line) and an orbit-following code prediction for the FEL case (solid line) have both been corrected for relativistic effects.

the FEL port relative to the Thomson scattering diagnostic and the time of the measurement relative to the FEL pulse. The nonrelativistic Thomson scattering spectrum was calculated from the distribution function, and a two-temperature relativistic correction was then applied to the model spectrum for comparison with the data [19]. Figure 3 shows good agreement between the theoretical model and the data, showing that the influence on the electron distribution function is as expected. A high-energy cutoff at ~15–20 keV predicted by theory is above the energy range of the Thomson measurements.

The presence of high-energy electrons was confirmed by the decay times of soft x rays and ECE which were typically $\simeq 20$ μs, corresponding to an energy of $\simeq 5$ keV if the energy loss is purely collisional. The multichannel soft x-ray array has nine vertical chords viewing from above; some chords had two detector channels with different Be filters (peak sensitivity at 5–7 keV) to provide information about the x-ray energy. The x-ray array was located at the FEL port for the insert data, and toroidally away from this port for the noninsert data. Code calculations [17] have shown that toroidal symmetry of the electron distribution is obtained on the order of 1 μs, comparable to the time resolution of the x-ray diagnostic, so the toroidal location is not expected to be important. Clear x-ray responses to the FEL were only observed after the tapered insert was installed (Fig. 1 is with the insert). The spatially localized response of the x rays seen in Fig. 1 is also consistent with the expected resonance width of $\simeq$1–1.5 cm. (Note in Fig. 1, the plasma axis is inside of the machine axis $r = 0$; this is consistent with x-ray, magnetic, and interferometer data.) Moving the resonance location by varying B_T has shown a corresponding relative change in the position of the x-ray signals. Because of the limited energy resolution of the x-ray diagnostic, detailed comparison with the theoretically predicted energy cutoff is not possible. However, the experimentally measured signal ratios from detectors with different Be filter thicknesses are not consistent with a large density of electrons at energies > 10 keV.

A limited set of experiments was performed to measure backscattered radiation that might provide information on the presence of the most worrisome parametric instabilities. The reflected microwave signals measured by a horn in the MTX port were below the receiver sensitivity, resulting in a ratio to the incident signal on the order of 10^{-5}. The receiver frequency was scanned 1.3 GHz downward from the FEL frequency with similar ratios, so we have no evidence of backscattered radiation. Brillouin backscattering is expected to be small because of the 20-ns FEL pulse length.

In summary, measurements in MTX demonstrated (1) increased transmission of high-power FEL pulses compared to low-power pulses, (2) the transmission is reduced (absorption is increased) when the gradient of $N_{||}$ of the beam is increased, (3) the on-axis FEL transmission decreases with increasing electron density, and (4) hot electrons are produced. These observations are in approximate quantitative agreement with theoretical models of the nonlinear ECRH interaction.

We would like to acknowledge the help from the Alcator Group at Massachusetts Institute of Technology (MTX was the Alcator-C tokamak at MIT). The LLNL FEL group, the JAERI team, and the MTX engineers and technicians were an integral part of the experiment. This work was performed under the auspices of the U.S. Department of Energy by the Lawrence Livermore National Laboratory under Contract No. W-7405-ENG-48.

[1] S.L. Allen and E.T. Scharlemann, in *Proceedings of the 9th International Conference on High Power Particle Beams, Washington, DC, May 1992* (IEEE, New York, 1992), p. 247.
[2] T.J. Orzechowski *et al.*, Nucl. Instrum. Methods Phys. Res., Sect. A **250**, 144 (1986).
[3] R.H. Cohen *et al.*, in *Nonlinear Phenomena in Vlasov Plasmas* (Editions de Physique, Orsay, France, 1989), p. 335.
[4] M.E. Fenstermacher *et al.*, in *Proceedings of the RF Power in Plasmas*, AIP Conf. Proc. No. 244 (AIP, New York, 1992), p. 20.
[5] B.W. Stallard *et al.*, Nucl. Fusion **30**, 2235 (1990).
[6] V.V. Alikaev *et al.*, in *Plasma Physics and Controlled Nuclear Fusion Research, 1986*, Proceedings of the 11th International Conference, Kyoto, 1986 (IAEA, Vienna, 1987), Vol. 1, p. 111.
[7] M. Bornatici *et al.*, Nucl. Fusion **23**, 1153 (1983).
[8] W.M. Nevins, T.D. Rognlien, and B.I. Cohen, Phys. Rev. Lett. **59**, 60 (1987).
[9] B.I. Cohen *et al.*, Rev. Mod. Phys. **63**, 949–990 (1991).
[10] T.J. Orzechowski *et al.*, Phys. Rev. Lett. **57**, 2172 (1986).
[11] S. L. Allen *et al.*, in *Plasma Physics and Controlled Fusion Research, 1991*, Proceedings of the 13th International Conference, Washington, 1990 (IAEA, Vienna, 1991), Vol. 1, p. 783.
[12] B.W. Stallard *et al.*, in *Proceedings of the 16th Symposium on Fusion Technology, London* (North-Holland, Amsterdam, 1990), Vol. 2, p. 1050.
[13] B. Felker and S.W. Ferguson, in *Proceedings of the 14th IEEE-NPSS Fusion and Engineering Symposium, San Diego* (IEEE, New York, 1991), p. 132.
[14] T. Oda *et al.*, Rev. Sci. Instrum. **61**, 2964 (1990).
[15] C.J. Lasnier *et al.*, in Proceedings of the 1993 IEEE Particle Accelerator Conference, Washington, DC (to be published).
[16] G.R. Smith, M.E. Fenstermacher, and E.B. Hooper, Nucl. Fusion **30**, 2505 (1990).
[17] T.D. Rognlien, Phys. Fluids **26**, 1545 (1983).
[18] R.H. Cohen and T.D. Rognlien, Phys. Fluids B **3**, 3406 (1991).
[19] J. Sheffield, *Plasma Scattering of Electromagnetic Radiation* (Academic, New York, 1975), p. 200.

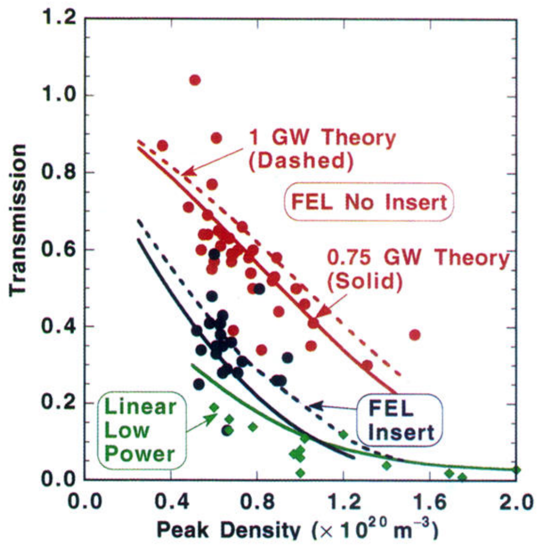

FIG. 2. The FEL high-power core transmission data (red circles) are greater than low-power data (green diamonds), demonstrating nonlinear absorption. Theoretical predictions of the FEL transmission without the insert (red: 1 GW, dashed; 0.75 GW, solid) compare well with the FEL data. An insert increases the $N_{\|}$ gradient of the microwave beam, thereby decreasing the experimentally measured transmission (blue circles), in agreement with nonlinear theory (blue: 1 GW, dashed; 0.75 GW, solid). The insert data and theory approach the linear theory (green line).